THE
EMBO
JOURNAL

Ribosomal position and contacts of mRNA in eukaryotic translation initiation complexes

Andrey V Pisarev[1,4], Victoria G Kolupaeva[1,4,5], Marat M Yusupov[3], Christopher UT Hellen[1] and Tatyana V Pestova[1,2,]*

[1]Department of Microbiology and Immunology, SUNY Downstate Medical Center, Brooklyn, NY, USA, [2]AN Belozersky Institute of Physico-Chemical Biology, Moscow State University, Moscow, Russia and [3]Institut de Génétique et de Biologie Moléculaire et Cellulaire, Illkirch, France

The position of mRNA on 40S ribosomal subunits in eukaryotic initiation complexes was determined by UV crosslinking using mRNAs containing uniquely positioned 4-thiouridines. Crosslinking of mRNA positions $+11$ to ribosomal protein (rp) rpS2(S5p) and rpS3(S3p), and $+9–+11$ and $+8–+9$ to h18 and h34 of 18S rRNA, respectively, indicated that mRNA enters the mRNA-binding channel through the same layers of rRNA and proteins as in prokaryotes. Upstream of the P-site, the proximity of positions $-3/-4$ to rpS5(S7p) and h23b, $-6/-7$ to rpS14(S11p), and $-8–-11$ to the 3′-terminus of 18S rRNA (mRNA/rRNA elements forming the bacterial Shine–Dalgarno duplex) also resembles elements of the bacterial mRNA path. In addition to these striking parallels, differences between mRNA paths included the proximity in eukaryotic initiation complexes of positions $+7/+8$ to the central region of h28, $+4/+5$ to rpS15(S19p), and -6 and $-7/-10$ to eukaryote-specific rpS26 and rpS28, respectively. Moreover, we previously determined that eukaryotic initiation factor2α (eIF2α) contacts position -3, and now report that eIF3 interacts with positions $-8–-17$, forming an extension of the mRNA-binding channel that likely contributes to unique aspects of eukaryotic initiation.

Introduction

During translation, mRNA engages in extensive, functionally important interactions with rRNA and protein components of the small ribosomal subunit, which determine the start site

*Corresponding author. Department of Microbiology and Immunology, SUNY Downstate Medical Center, 450 Clarkson Avenue, Box 44, Brooklyn, NY 11203, USA. Tel.: +718 2216121; Fax: 718 2702656; E-mail: tatyana.pestova@downstate.edu
[4]These authors contributed equally to this work
[5]Present address: Department of Microbiology, New York University School of Medicine, New York, NY 10016, USA

for initiation and ensure the accuracy of tRNA selection during elongation. The path of mRNA on the prokaryotic 30S subunit has been visualized by X-ray crystallography of ribosomal complexes that correspond to different states in translation (Yusupova *et al*, 2001, 2006; Jenner *et al*, 2005, 2007; Selmer *et al*, 2006; Korostelev *et al*, 2007). Thus, mRNA is threaded through a channel that wraps around the neck of the 30S subunit, passing through non-covalently closed tunnels as it enters between the head and shoulder and as it exits between the head and platform, leaving only nts $-1–+7$ (relative to the $+1$ A of the AUG initiation codon) exposed on the interface surface. The A- (aminoacyl) and P (peptidyl)-site codons are centred over the axis of helix 44 of 16S rRNA, and a kink between them allows simultaneous pairing with the anticodons of A- and P-site tRNAs without steric clashes. mRNA nts $+7–+15$ pass through rRNA (h34, h28, the 5′ hairpin loop and the 530 loop) and ribosomal protein ((rp) S3p, S4p and S5p) layers of the narrow entry tunnel. However, the contact between the head and the body formed between h18 in the body and h34 and S3p in the neck, which constitutes part of the mRNA entry tunnel, was observed in 70S ribosomes and in some but not all 30S subunit structures (e.g. Frank *et al*, 1995; Clemons *et al*, 1999; Gabashvili *et al*, 1999; Schluenzen *et al*, 2000), indicating that it can potentially function as a 'latch'. It has been suggested that closing of the tunnel could contribute to processivity and directionality, whereas the open conformation could facilitate ribosomal attachment of mRNA during initiation (Schluenzen *et al*, 2000). The interactions of mRNA with the 30S subunit upstream of the P-site codon differ at the various stages of translation. In initiation complexes, mRNA nts $-5–-12$ base pair with 16S rRNA to form the Shine–Dalgarno (SD) duplex located in a cleft formed by S11p, S18p and h20, h28, h37 and the 723 bulge loop of 16S rRNA, and is oriented towards S18p. Nucleotides $-1–-4$ containing the E-site codon are positioned in the short exit tunnel between the head and platform and are surrounded by S7p, h45, h28, and the 690 and 790 loops of 16S rRNA. In the post-initiation state, initial elongation cycles result in lengthening of the SD duplex and its reorientation towards S2p. Further translation leads to melting of the SD duplex and loss of stable interactions of the ribosome with mRNA upstream of position -5. The E-site nucleotides $-1–-3$ are positioned on top of a bulge between h44 and h45 and near h24 in initiation and post-initiation complexes, but have an altered conformation in the latter, adopting an A-helical shape that can base pair with the E-site tRNA, and no longer interact with S7p. During the first stage in initiation, mRNA binds prokaryotic ribosomes by forming the SD duplex, which is oriented towards S2p as in post-initiation complexes, whereas the rest of mRNA is still unbound.

By contrast, much less is known about the mRNA path on eukaryotic ribosomes. There are fundamental mechanistic differences between eukaryotes and prokaryotes in initial ribosomal attachment of mRNA and selection of the initiation codon (Pestova *et al*, 2007), so that knowledge of the

ribosomal position of mRNA and its functional contacts with components of the 40S subunit and with eukaryotic initiation factors (eIFs) at different stages of initiation are of particular interest. Ribosomal attachment to eukaryotic mRNAs is mediated by eIFs instead of by the SD interaction. Moreover, in contrast to 30S subunits that directly attach to the initiation codon region of prokaryotic mRNAs, eukaryotic 43S preinitiation complexes (comprising a 40S subunit, eIF2·GTP/Met-tRNA$_i^{Met}$, eIF3, eIF1 and eIF1A) first attach to the capped 5′-proximal region of mRNA and then scan along the 5′-untranslated region (5′-UTR) to the initiation codon where they form 48S initiation complexes with established P-site codon–anticodon base pairing. Initial attachment of 43S complexes is mediated by eIF4F, eIF4A and eIF4B. eIF4F comprises eIF4E (cap-binding protein), eIF4A (a helicase, whose activity is enhanced by eIF4B) and eIF4G (a scaffold for eIF4E and eIF4A that also binds eIF3). eIFs 4F, 4A and 4B unwind the cap-proximal region of mRNA and likely promote attachment of 43S complexes through the eIF3–eIF4G interaction. The location of eIF4A/4B/4F on the 40S subunit is unknown, and the molecular mechanism by which mRNA bound to eIF4F enters the mRNA-binding cleft therefore remains unresolved. Subsequent scanning requires eIF1, which promotes adoption of a scanning-competent conformation by 43S complexes and enables them to recognize and reject codon–anticodon mismatches (Pestova and Kolupaeva, 2002; Lomakin *et al*, 2003, 2006). However, the molecular mechanism of scanning, the ribosomal position of mRNA in scanning 43S complexes and its potential contacts with eIFs in these complexes, as well as the mechanism by which eIF4A/4B/4F assist scanning remain unknown. Initiation codon recognition in metazoans is strongly influenced by flanking nucleotides: the sequence GCC(**A/G**)CC<u>AUG</u>**G** (in which the initiation codon is underlined) is optimal for initiation, and deviations from it at the $^-3$ and $^+4$ positions (in bold) lead to initiation at the next downstream AUG triplet by leaky scanning (Kozak, 1991). eIF1 is also responsible for the ability of 43S complexes to discriminate against AUG codons in poor context (Pestova and Kolupaeva, 2002; Pisarev *et al*, 2006). Purines at the $^+4$ and $^-3$ positions interact specifically with AA$_{1818–1819}$ of 18S rRNA and with the eIF2 α-subunit, respectively, and it was proposed that these interactions may stabilize conformational changes that likely occur in ribosomal complexes upon initiation codon recognition (Pisarev *et al*, 2006). After 48S complexes have formed, eIF5 triggers hydrolysis of eIF2-bound GTP, and eIF5B then mediates displacement of factors from the 40S subunit and joining with a 60S subunit, yielding an elongation-competent 80S initiation complex.

The position of mRNA on the 40S subunit, as well as its interactions with translation components, except those of nucleotides at positions $^-3$ and $^+4$, is not known for ribosomal complexes at any stage of initiation. RNAse protection studies have shown that, similarly to prokaryotic 70S ribosomes, eukaryotic 80S ribosomes also protect ∼30 nt of mRNA, but that 48S complexes bind an additional 10–20 nt of mRNA on its 5′-side, likely through eIFs (Kozak, 1977; Lazarowitz and Robertson, 1977). These additional contacts outside the mRNA-binding cleft could be important for ribosomal attachment to or scanning on mRNA. The ribosomal position of mRNA in initiation complexes upstream of the P-site is particularly interesting also because eukaryotes lack

the SD interaction. To gain insights into the architecture of eukaryotic initiation complexes, we characterized in detail the ribosomal position of mRNA and its specific interactions with eIFs in a stable assembly intermediate, the 48S initiation complex, and in the final assembly product, the 80S initiation complex, by site-directed zero-length UV crosslinking using a panel of mRNAs containing 4-thiouridines (4^SU) at unique positions from $^-26$ to $^+11$ relative to the initiation codon. The obtained data are compared with the path of mRNA on the prokaryotic 30S subunit.

Results

Contacts of mRNA with rps and initiation factors in 48S and 80S initiation complexes

To define the path of mRNA on the 40S subunit and to identify specific interactions of mRNA with the components of initiation complexes assembled by scanning-mediated initiation, a panel of mRNAs was employed that contained uridines at single unique positions from $^-26$ to $^+11$ relative to the A of the initiation codon in addition to the uridine ($^+2$) in the initiation codon (Table I; Figure 1A). Initiation codons were flanked by ∼30-nt-long sequences comprising multiple CAA triplets to minimize secondary structure and increase initiation efficiency. mRNAs were transcribed *in vitro* in the presence of [α-^{32}P]ATP and 4^SU, which can be specifically crosslinked to proteins and nucleic acids by low-energy (360 nm) irradiation, yielding 'zero-length' crosslinks (Favre *et al*, 1998) that represent direct contacts of the nucleotide with 48S complex constituents. As discussed elsewhere (Sergiev *et al*, 2001a, b; Yusupova *et al*, 2001), interactions of mRNA with prokaryotic ribosomes revealed using this method correlate well with the crystal structures of the mRNA/70S ribosome complex. The presence of 4^SU in the 5′-UTR of an mRNA does not impair ribosomal scanning and the efficiency of 48S complex formation (Pisarev *et al*, 2006). 48S complexes were assembled from 40S subunits, eIFs 1, 1A, 3, 4A, 4B, 4F and eIF2·GTP·Met-tRNA$_i^{Met}$. To form 80S initiation complexes, reaction mixtures were supplemented with 60S subunits, eIF5 and eIF5B. Initiation complexes were purified by sucrose density gradient centrifugation and irradiated. After crosslinking, ribosomal complexes were subjected to a second round of sucrose density gradient centrifugation, because a small proportion of them dissociate during the procedure, leading to nonspecific crosslinking of released mRNA with mRNA-binding components of initiation complexes (e.g. eIF3). To identify crosslinked proteins, purified initiation complexes were treated with RNases and analysed by SDS–PAGE and two-dimensional (2D) gel electrophoresis. This technique previously allowed us to identify specific interactions in 48S complexes of the nucleotide at position $^-3$ of mRNA with eIF2α and rpS5 (S7p), and of the $^+4$ nucleotide with rpS15 (S19p) (Pisarev *et al*, 2006, 2007).

The 4^SU residue that was present in all mRNAs at position $^+2$ in the initiation codon is base paired with the initiator tRNA anticodon and therefore should not crosslink to other components of initiation complexes. Consistently, no crosslinking with eIFs or rps was observed for control mRNA that contained 4^SU only at this position (Figure 1B, lane 12), whereas crosslinking to mRNAs containing 4^SU at additional positions yielded specific crosslinking patterns (Figures 1B and C; summarized in Figure 1G, compared to the contacts of

Table I Sequences of mRNAs used for UV crosslinking

	mRNA transcript (positions of U's)	Sequences
1	−26, +2	G*U*AA(CAA)7CC<u>AUG</u>A(CAA)9CGGCC
2	−17, +2	G(CAA)3*U*AA(C<u>AA</u>)4CC<u>AUG</u>A(CAA)9CGGCC
3	−14, +2	G(CAA)4*U*AA(CAA)3CC<u>AUG</u>A(CAA)9CGGCC
4	−11, +2	G(CAA)5*U*AA(CAA)2CC<u>AUG</u>A(CAA)9CGGCC
5	−10, +2	G(CAA)6C*U*A(CAA)2CC<u>AUG</u>A(CAA)9CGGCC
6	−8, +2	G(CAA)6*U*AACAACC<u>AUG</u>A(CAA)9CGGCC
7	−7, +2	G(CAA)7C*U*ACAACC<u>AUG</u>A(CAA)9CGGCC
8	−6, +2	G(CAA)6CA*U*CAACC<u>AUG</u>A(CAA)9CCC
9	−5, +2	G(CAA)7*U*AACC<u>AUG</u>A(CAA)9CCC
10	−4, +2	G(CAA)8C*U*ACC<u>AUG</u>A(CAA)9CGGCC
11	−3, +2	A(CAA)8CA*U*CC<u>AUG</u>A(CAA)9CCC
12	−2, +2	G(CAA)8*U*C<u>AUG</u>A(CAA)9CCC
13	+2	G(CAA)3CAC<u>C</u>A<u>UG</u>A(CAA)8CGGCC
14	+4, +2	ACAA9CC<u>AUG</u>*U*(CAA)9CCC
15	+5, +2	G(CAA)3CAC<u>C</u>A<u>UG</u>A*U*(CAA)8CGGCC
16	+6, +2	G(CAA)8CC<u>AUG</u>AC*U*A(CAA)8CCC
17	+7, +2	G(CAA)8C<u>C</u>A<u>UG</u>ACA*U*(CAA)8CCC
18	+8, +2	G(CAA)3CAC<u>C</u>A<u>UG</u>ACAA*U*(CAA)7CGGCC
19	+9, +2	G(CAA)8CC<u>AUG</u>ACAAC*U*A(CAA)7CCC
20	+10, +2	G(CAA)8CC<u>AUG</u>ACAACA*U*(CAA)7CCC
21	+11, +2	G(CAA)3CAC<u>C</u>A<u>UG</u>A(CAA)2*U*(CAA)6CGGCC
22	−14, −8, −4, +2, +5, +11	G(CAA)5*U*AACAA*U*AAC*U*ACC<u>AUG</u>A*U*AACAA*U*AA(CAA)6CGGCC

The AUG initiation codons are underlined and the positions at which 4^SU residues were incorporated are bold and italicized.

mRNA nucleotides with ribosomal proteins in the mRNA/ *Thermus thermophilus* 30S subunit in Figure 1H and mapped onto the crystal structure of the mRNA/*T. thermophilus* 30S subunit complex in Figure 5). In 48S complexes, nucleotides at positions from −17 to +11 crosslinked to several proteins with molecular weights ranging from ∼6 to ∼32 kDa (Figure 1B, lanes 2–11). The low molecular weights of crosslinked proteins and the fact that the same crosslinking pattern for each individual position was observed in 48S (Figure 1B) and in 80S initiation complexes (Figure 1C) indicated their ribosomal nature. They were attributed to distinct rps by 2D gel electrophoresis taking into consideration the 'northwest' shift caused by covalently bound mRNA nucleotides, whose identity was then confirmed by mass-spectrometry sequencing of tryptic peptides (Supplementary Table 1). To simplify presentation of 2D gel analysis, we assembled 48S complexes on mRNA that simultaneously contained 4^SU at positions −14, −8, −4, +5 and +11 (Figure 1D), because crosslinking to 4^SU at these positions (Figure 1E) covered the whole spectrum of rps that crosslink to individual mRNA positions from −26 to +11 (see below). Therefore, instead of showing numerous 2D gels that correspond to each individual 4^SU position, we have presented a summarizing 2D gel for crosslinking of mRNA containing 4^SU at positions −14, −8, −4, +5 and +11 (Figure 1F), and will discuss the crosslinking of individual positions using one-dimensional gels (Figures 1B and C) as illustrations.

Thus, on the A-site side of the 40S subunit, mRNA crosslinked to rpS2 (the eukaryotic homologue of S5p), rpS3 (S3p) and rpS15 (S19p). rpS2 and rpS3 crosslinked most strongly to position +11 and much less so to positions +8–+10 (Figure 1B, lanes 10 and 11; Figure 1C, lanes 10–13). The crosslinking intensity of rpS2 (the upper of the two closely migrating bands in lanes 10–13 of Figures 1C and F) was substantially weaker than that of rpS3 (the lower of these bands; Figure 1C, lanes 10–13; Figure 1F). rpS15 crosslinked to position +5 (Figure 1B, lane 9; Figure 1C, lane 8; Figure 1F) and as previously reported, also to position +4

(Pisarev *et al*, 2006). On the E-site side of the 40S subunit, mRNA crosslinked to rpS5 (S7p), rpS14 (S11p), rpS28 and rpS26. rpS5 crosslinked to positions from −3 to −5, with maximal efficiency to position −3 (Figure 1B, lane 8; Figure 1C, lanes 4–6; Figure 1F). rpS14 crosslinked to positions −6–−8, with the highest intensity to positions −6/−7 (the upper band in Figure 1C, lanes 1–3, and the upper of the two closely migrating bands in Figure 1B, lanes 6 and 7). rpS28 crosslinked to positions −4–−8, with the highest intensity to position −6 (the lowest band in Figure 1B, lanes 6–8 and Figure 1C, lanes 1–5). rpS26 crosslinked to positions −7–−14, with the highest intensity to positions −7–−10 (Figure 1B, lanes 2–7; Figure 1C, lanes 1 and 2). No rps crosslinked to positions −26, −2 or +7 (Figure 1B, lane 1; Figure 1C, lanes 7 and 9). Figure 1F is a summarizing 2D electrophoresis gel illustrating crosslinking in 48S complexes of all seven rps to mRNA simultaneously containing 4^SU at positions −14, −8, −4, +5 and +11. Taking into account the 'northwest' shift of crosslinked proteins, it is clearly seen that this mRNA crosslinks to rpS2 (through position +11), rpS3 (through position +11), rpS5 (through position −4), rpS15 (through position +5), rpS14 (through position −8), rpS26 (through positions −8 and −14) and rpS28 (through positions −4 and −8). The radioactive spot that almost co-migrated with rpS21 (bottom left corner in both panels of Figure 1F) most likely corresponds to crosslinked rpS28 bound to additional undigested nucleotide(s), thus accounting for the greater shift.

UV crosslinking of 48S complexes also revealed that in addition to the previously reported crosslinking of eIF2α to 4^SU or 6^SG at position −3 (Pisarev *et al*, 2006), mRNA on the E-site side of the 40S subunit also interacts extensively with eIF3, yielding a distinctive pattern of radiolabelled eIF3 subunits that crosslink to positions −8–−17 (Figure 1B, lanes 2–6). The most intense crosslinking was between eIF3a and 4^SU at position −14 (Figure 1B, lane 3). eIF3a also crosslinked to position −17 albeit less strongly (Figure 1B, lane 2). eIF3d crosslinked to 4^SU at positions −8, −10, −11, −14 and −17 with very similar intensities

Figure 1 Contacts of mRNA with ribosomal proteins and initiation factors in 48S/80S initiation complexes identified by UV crosslinking. (**A**) Structure of mRNAs employed for UV crosslinking. The positions of unique uridines relative to the initiation codon are indicated by asterisks underneath the sequence. (**B, C**) Crosslinking of ^{32}P-labelled mRNAs containing 4^{S}U at indicated positions with components of 48S (**B**) and 80S (**C**) initiation complexes assayed by SDS–PAGE and autoradiography. Separation of lanes in (B) by white lines indicates that they were derived from three separate gels that were run under the same conditions. The positions of molecular weight (MW) markers are shown on the left. The crosslinked ribosomal proteins and eIF3 subunits are indicated on the right. (**D**) 48S complex formation on mRNA simultaneously containing 4^{S}U at positions $^-$14, $^-$8, $^-$4, $^+$5 and $^+$11 assayed by toe printing. The positions of uridines, of the AUG codon, of full-length cDNA and of toe prints that correspond to 48S complexes are indicated. Lanes C, T, A and G depict corresponding cDNA sequences. (**E**) Crosslinking of ^{32}P-labelled mRNAs containing 4^{S}U at positions $^-$14, $^-$8, $^-$4, $^+$5 and $^+$11 with components of 48S complexes assayed by SDS–PAGE and autoradiography. (**F**) Analysis by 2D electrophoresis of ribosomal proteins crosslinked to ^{32}P-labelled mRNAs containing 4^{S}U at positions $^-$14, $^-$8, $^-$4, $^+$5 and $^+$11. The panel on the left shows 2D gel stained with Simply Blue Safe Stain; the panel on the right shows an autoradiograph of the same gel. Positions corresponding to radioactive spots on the right panel are shown in red in the left panel. Red arrows indicate the 'northwest' shift. The positions of ribosomal proteins based on sequencing data (Supplementary Table 1) or according to Madjar *et al* (1979) are indicated on the left panel. (**G**) A diagram summarizing the strongest contacts of ribosomal proteins and eIFs with mRNA nucleotides at different positions in 48S/80S initiation complexes. (**H**) Contacts of mRNA nucleotides at different positions with ribosomal proteins on the prokaryotic 30S subunit in the crystal structure of the mRNA/*T. thermophilus* 30S subunit complex (Yusupova *et al*, 2001).

(Figure 1B, lanes 2–6). Crosslinking of eIF3b to positions $^-14$, $^-17$ and $^-26$ was not consistently significantly over the background (Figure 1B, lanes 1–3; data not shown), and we are therefore reluctant to suggest that crosslinking of eIF3b was specific. No labelling of other eIFs by crosslinking to mRNA was detected.

Contacts of mRNA with 18S rRNA in 48S and 80S initiation complexes

Sites of crosslinking in 18S rRNA of 4^SU at different positions in mRNA were identified in two stages. First, the approximate region of crosslinking was determined by RNase H mapping (Dontsova et al, 1992). For this, 18S rRNA was extracted from irradiated 48S/80S initiation complexes, hybridized with DNA oligonucleotides complementary to different regions, incubated with RNase H and resolved by gel electrophoresis. Attribution of ^{32}P-labelled UV crosslinked fragments of 18S rRNA took into account their reduced mobility due to the covalently linked ~ 70-nt-long mRNA. In the second stage, the exact crosslinked nucleotide in 18S rRNA was identified by primer extension inhibition using a primer chosen on the basis of RNase H mapping. The positions of crosslinked nucleotides in rabbit 18S rRNA are shown in Figure 3A, summarized in Figure 3B and mapped onto the crystal structure of the mRNA/T. thermophilus 30S subunit complex in Figure 6.

As in the case of rps, crosslinking of individual mRNA positions to 18S rRNA was identical in 48S and 80S initiation complexes. Therefore to simplify presentation, only gels that represent crosslinking in 48S complexes are shown (Figure 2). 4^SU at position $^-17$ crosslinked to nts 1085–1113 of 18S rRNA (Figure 2A, lane 3). Primer extension analysis identified the crosslinked nucleotide as U_{1107} of h26 (Figure 2B, lane 1). The control experiment (Figure 2B, lane 2) was done using 48S complexes assembled on mRNA containing 4^SU only at position $^+2$ in the initiation codon. Position $^-14$ also crosslinked to nts 1085–1113 (data not shown) but so weakly that precise identification of the crosslinking site by primer extension was impossible, suggesting that position $^-14$ mainly interacts with eIF3a (Figure 1B, lane 3). Positions $^-11$–$^-8$ crosslinked to the 3'-terminal nts 1857–1863 of 18S rRNA (Figures 2C and D; data not shown). No substantial crosslinking with 18S rRNA was detected for position $^-7$ (data not shown). Position $^-4$ crosslinked to overlapping regions corresponding to nts 912–972 and 947–1052 (Figure 2E, lanes 2 and 3), suggesting that the crosslinking site lay within 26 nt between nts 947–972 of the apical part of h23, but the intensity of crosslinking was too low for unambiguous identification of the exact crosslinking site. Positions $^+7$ and $^+8$ crosslinked to nts 1676–1699 (Figure 2F, lanes 2 and 3); primer extension identified the crosslinked nucleotides as $CUUUGUA_{1684-1690}$ and A_{1692} of h28 (Figure 2G, lanes 3 and 4). Crosslinking to $CU_{1684-1685}$ was most efficient. Very weak crosslinking to these positions was also observed for the flanking $^+6$ and $^+9$ positions (Figure 2F, lanes 1 and 4; Figure 2G, lanes 2 and 5). Medium intensity crosslinking occurred between positions $^+8/^+9$ and C_{1484} of h34 (Figure 2G, lanes 2 and 3). 4^SU at $^+9$–$^+11$ positions crosslinked to nts 489–662 (Figure 2H, lanes 2–4), and primer extension analysis identified the crosslinked nucleotides as U_{617} and A_{619} of h18 (Figure 2I, lanes 3–5). Position $^+10$ crosslinked more efficiently than at positions $^+9$ and $^+11$, and crosslinking of A_{619} was more intense than that of U_{617}.(Figures 3A and B)

In conclusion, these results indicate that on the E-site side of the 40S subunit, mRNA is close to h26, the seven 3'-proximal nucleotides and the apical region of h23, whereas on the A-site side of the 40S subunit, mRNA contacts nucleotides in h28, h34 and h18, and as previously reported, in the base of h44 (Pisarev et al, 2006).

Interactions of eIF3 with the 40S subunit

The crosslinking pattern of eIF3 subunits with mRNA positions $^-8$–$^-17$ suggests that eIF3d and eIF3a likely interact with elements of the 40S subunit that form the mRNA-binding channel. To gain additional insights into the ribosomal position of eIF3, we used the complementary approaches of chemical/enzymatic footprinting and directed hydroxyl radical cleavage of 18S rRNA in 40S/eIF3 complexes. eIF3 binds stably to 40S subunits in the presence of poly(U) (Kolupaeva et al, 2005). Assembled eIF3/poly(U)/40S subunit complexes were separated from unincorporated components by sucrose density gradient centrifugation and subjected to limited digestion with RNase T1 (which cleaves RNA after unpaired G residues) or RNase V1 (which cleaves double-stranded RNA without base specificity), or treated with N-cyclohexyl-N'-(2-morpholinoethyl)-carbodiimide methyl-p-toluene sulphonate (CMCT), which modifies unpaired uracil and to a lesser extent guanine residues. Consistent with eIF3's binding to the protein-rich solvent side of the 40S subunit (Siridechadilok et al, 2005), eIF3 protected very few sites in 18S rRNA from enzymatic cleavage. The strongest protection was in h16. Thus, eIF3 protected G_{537} from RNase T1 cleavage (Figure 4A, lanes 1 and 2; Figure 4D) and the nearby C_{539} from RNase V1 cleavage (Figure 4B, lanes 2 and 3; Figure 4D). Protection at the same sites was observed in 43S complexes that contained 40S subunits, eIF3 and eIF2 ternary complex (data not shown). Interestingly, eIF3 did not protect $UUU_{530-532}$ in the apical loop of h16 (Figure 4A, lanes 3 and 4), which suggests that eIF3 either interacts with the stem but not the apical loop of h16, or that it does not directly interact with h16 but binds closely enough to block access of RNases but not of the smaller CMCT molecule. However, it is also possible that protection from enzymatic cleavage resulted from conformational changes in 40S subunits induced by factor binding rather than from direct interaction between h16 and eIF3.

The footprinting approach was complemented by directed hydroxyl radical probing (Culver and Noller, 2000; Lomakin et al, 2003; Unbehaun et al, 2007), in which locally generated hydroxyl radicals cleave 18S rRNA in the vicinity of Fe(II) tethered to cysteine residues on the surface of eIF3 through the linker 1-(p-bromoacetamidobenzyl)-EDTA (BABE). Native eIF3 contains 65 cysteine residues, some of which might be surface-exposed and could therefore be conjugated with Fe(II)–BABE. Derivatization of eIF3 did not affect its activity in 48S complex formation (data not shown), and cleavage of 18S rRNA was therefore analysed in 40S/[Fe(II)–BABE]–eIF3/poly(U) and 43S complexes. Medium intensity cleavage occurred at $GC_{537-538}$ of h16 (Figure 4C, lanes 1 and 2; Figure 4D; data not shown). This site coincides with sites of protection by eIF3 from RNase digestion (Figures 4A and B). Although protection from enzymatic cleavage could theoretically be the result of conformational changes in rRNA
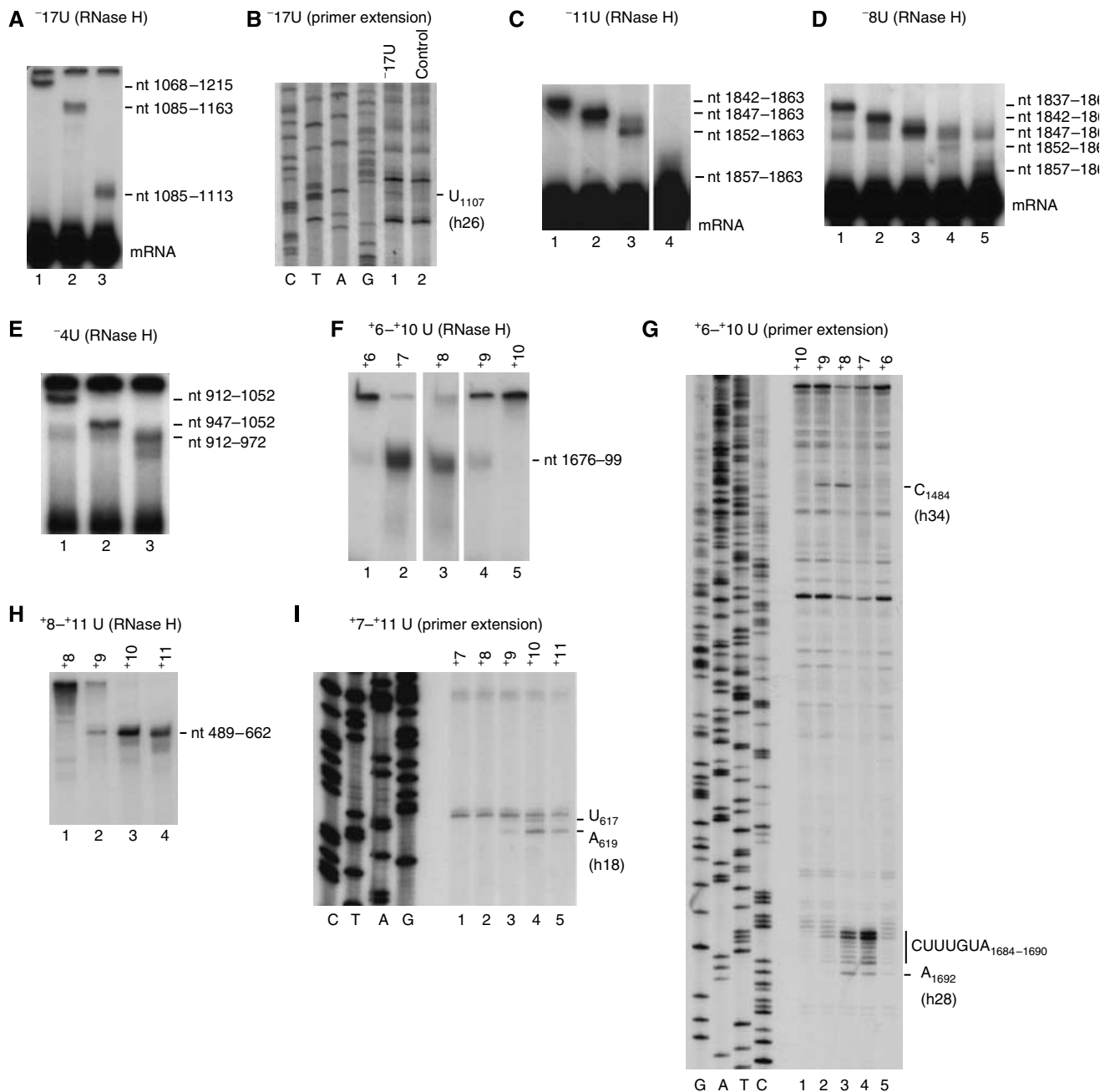
Figure 2 Contacts of mRNA with 18S rRNA in 48S complexes identified by UV crosslinking. (**A**, **C**–**F**, **H**) RNase H digestion of 18S rRNA crosslinked to ^{32}P-labelled mRNAs containing 4^SU at indicated positions in 48S complexes. 18S rRNA was digested with RNase H and DNA primers complementary to different regions and analysed by denaturing PAGE and autoradiography. White lines separate lanes 3 and 4 (C) and lanes 2–4 (F), which were juxtaposed from the same gel (C) or derived from two separate gels that were run under the same conditions (F). 18S rRNA fragments, to which mRNAs had crosslinked, are shown on the right. The position of free uncrosslinked mRNA is also shown in (A, C, D). (**B**, **G**, **I**) Determination of exact sites of crosslinking by primer extension analysis. The positions of RT stop sites are indicated on the right. Lanes C, T, A and G depict sequences of mouse (B, I) or *Xenopus* (G) 18S rRNA.

induced by factor binding, the fact that h16 was also cleaved by hydroxyl radicals strongly suggests that eIF3 is located at least near this region of the 40S subunit.

Discussion

The results of UV crosslinking experiments presented here and elsewhere (Pisarev *et al*, 2006) have revealed striking parallels between the path of mRNA in eukaryotic initiation complexes and on the prokaryotic ribosome, as well as

differences, some of which likely reflect unique aspects of eukaryotic initiation. We will compare the data obtained in the present study with the crystallographically visualized mRNA path on the *T. thermophilus* ribosome containing P- and E-site tRNAs (Yusupova *et al*, 2001, 2006; Figures 5 and 6), and with previously reported crosslinking data for pro- karyotic 70S ribosomal complexes obtained using the same zero-length crosslinking technique as employed here and for eukaryotic 80S ribosomal complexes phased by cognate tRNA obtained using mid-range nucleotide derivatives.
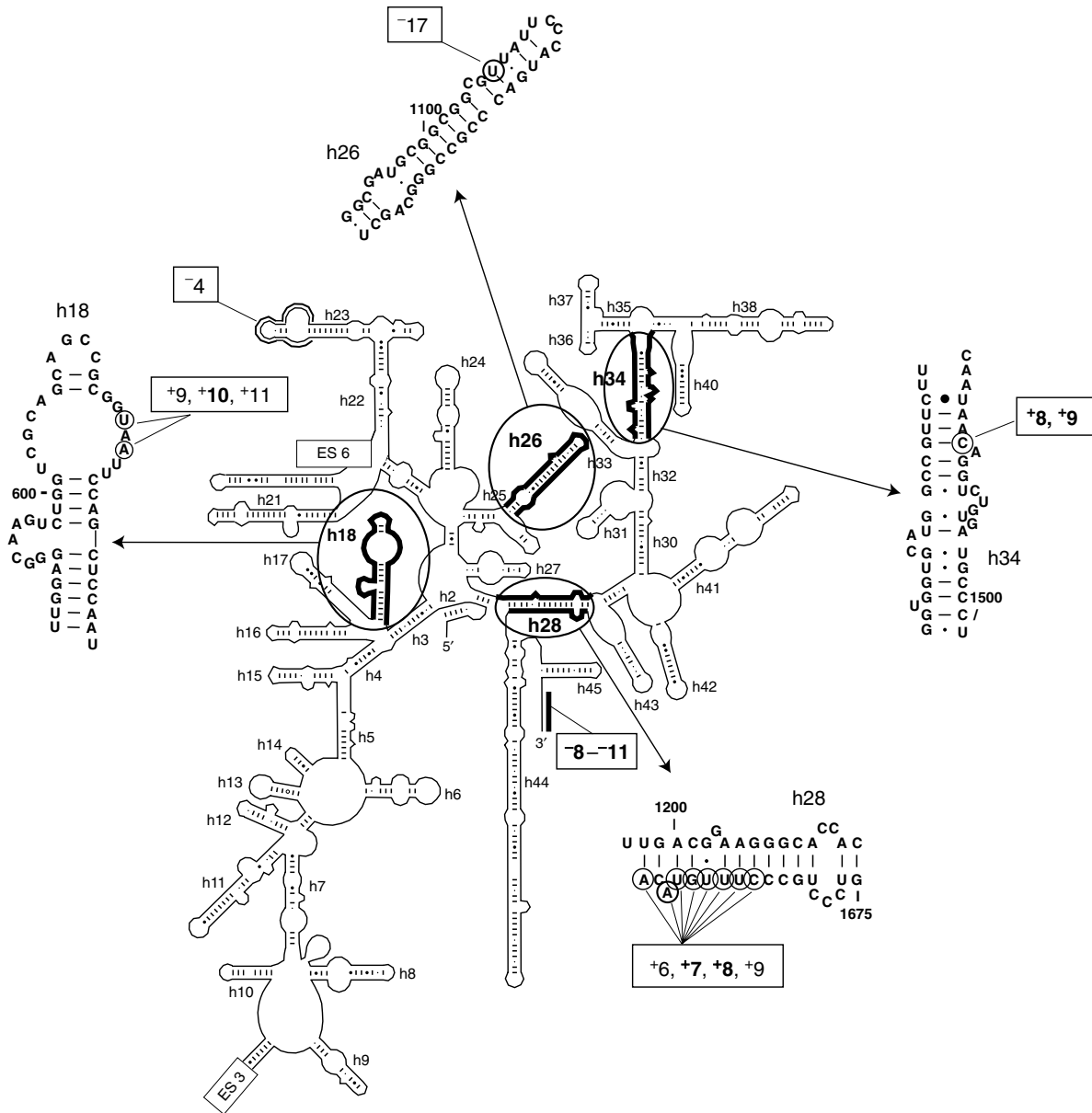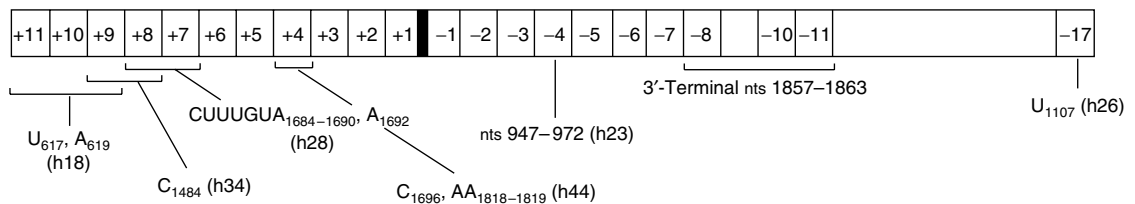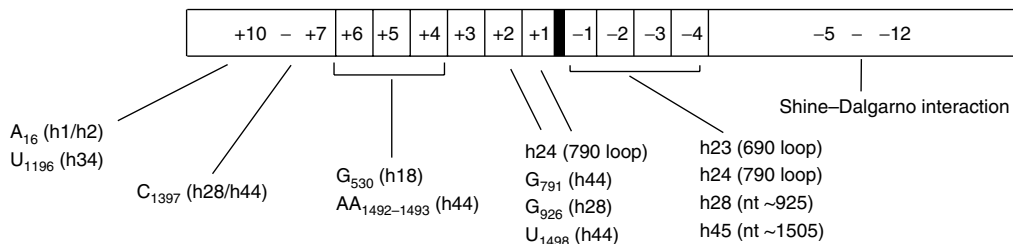
Figure 3 Summary of contacts of mRNA nucleotides with 18S rRNA in 48S/80S initiation complexes. (**A**) Sites of crosslinking of different mRNA positions in 48S/80S complexes mapped onto the secondary structure of 18S rRNA. Crosslinking sites are either shown as bars on the secondary structure of 18S rRNA (for positions ⁻4 and ⁻8–⁻11) or circled on close-up views of named rRNA elements. The corresponding mRNA positions are shown in boxes. (**B**) A diagram summarizing contacts of mRNA at different positions with 18S rRNA in 48S/80S initiation complexes. (**C**) Contacts of mRNA nucleotides at different positions with 16S rRNA of the prokaryotic 30S subunit in the crystal structure of the mRNA/*T. thermophilus* 30S subunit complex (Yusupova *et al*, 2001).
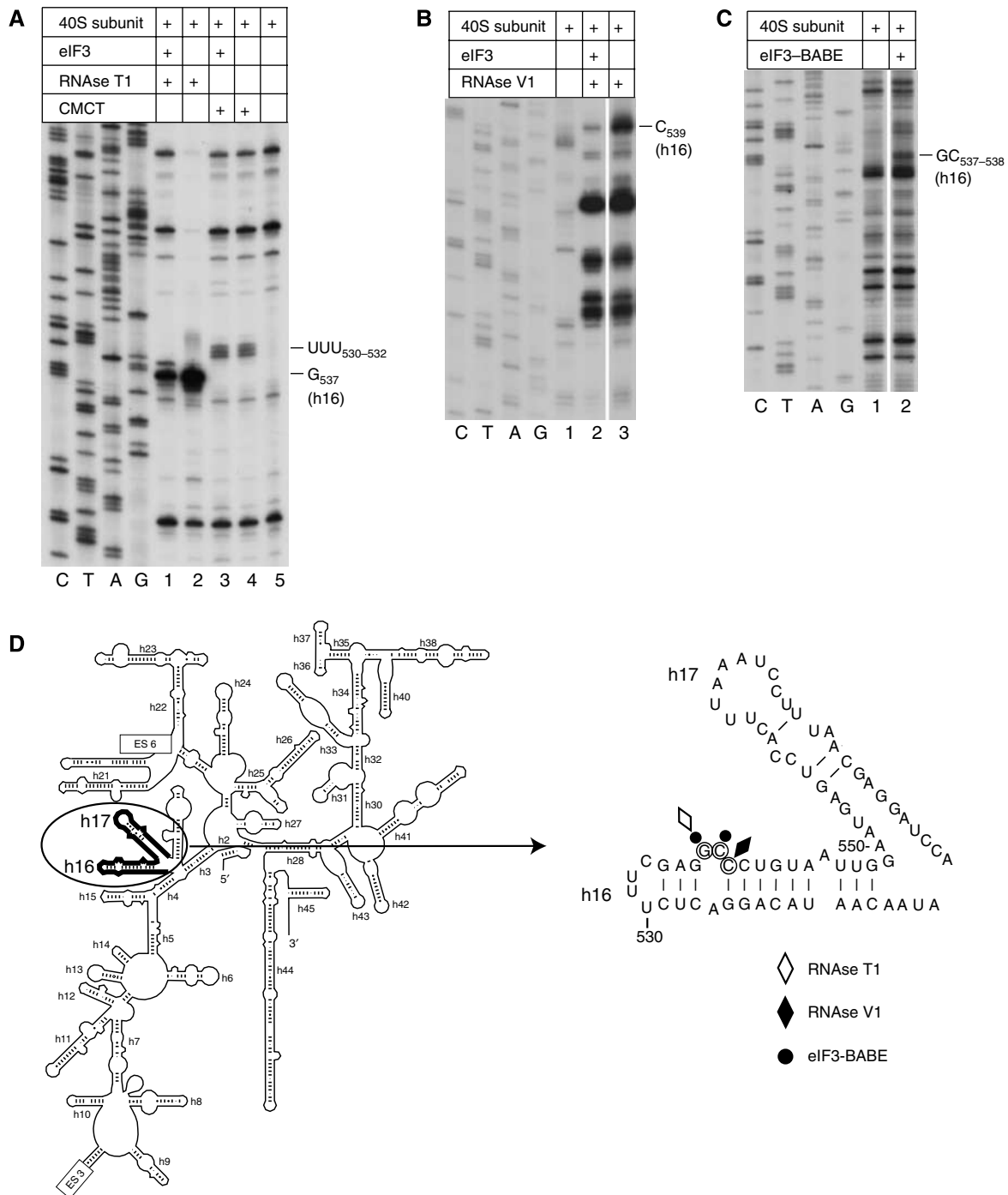
Figure 4 Enzymatic footprinting and directed hydroxyl radical cleavage of 18S rRNA in eIF3/40S subunit complexes. (**A, B**) Enzymatic and chemical footprinting analysis of 18S rRNA in eIF3/40S subunit complexes. Fractionation of cDNA products obtained after primer extension shows the sensitivity of 18S rRNA to cleavage by RNAses T1 (A) and V1 (B) or to modification by CMCT (A) in 40S subunit alone or in complex with eIF3. The positions of residues protected by eIF3 from RNase digestion or modified by CMCT are shown on the right. Lanes C, T, A and G depict the sequence of mouse 18S rRNA. (**C**) Hydroxyl radical cleavage of 18S rRNA from Fe(II) tethered to cysteines on the surface of native eIF3 in eIF3/40S subunit complexes. Sites of cleavage were mapped by primer extension inhibition. The positions of cleaved nucleotides are shown on the right. Lanes C, T, A and G depict the sequence of mouse 18S rRNA. White lines separate lanes 2 and 3 (B) and lanes 1 and 2 (C), which in both cases were juxtaposed from the same gel. (**D**) Sites of protection from RNase T1 and RNase V1 digestion and of directed hydroxyl radical cleavage in eIF3/40S subunit complexes mapped onto the secondary structure of 18S rRNA. Protection and cleavage sites are circled in a close-up view of h16.

Ribosomal position and contacts of mRNA downstream of the P-site

Efficient UV crosslinking of mRNA at position $^{+}11$ to rpS2 and rpS3 (homologues of S5p and S3p, respectively) indicates that mRNA enters the mRNA-binding channel of eukaryotic ribosomes through the same layer of proteins as in prokaryotic ribosomes.

UV crosslinking of positions $^{+}9$–$^{+}11$ to h18 (U_{617} and A_{619}) and of $^{+}8/^{+}9$ to h34 (C_{1484}) was consistent with the proximity of this region to the 530 loop of h18 and to U_{1196} of
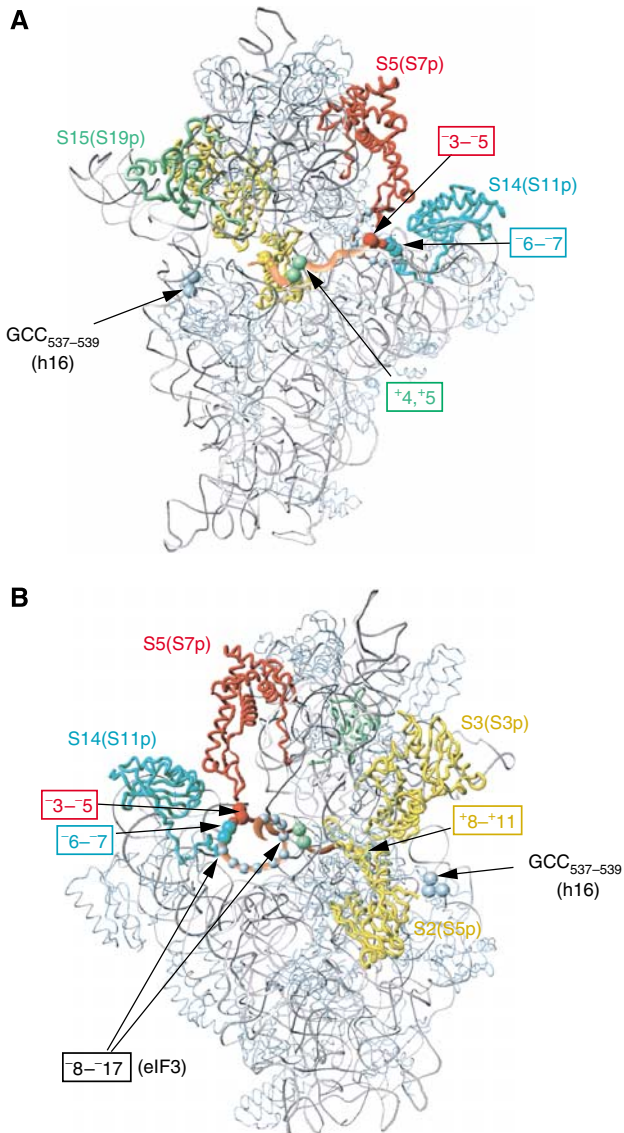
Figure 5 Ribosomal proteins crosslinked to different positions of mRNA in 48S/80S initiation complexes mapped onto the crystal structure of the mRNA/*T. thermophilus* 30S subunit complex (Yusupova *et al*, 2006; PDB code 2HGR): (**A**) intersubunit side view and (**B**) solvent side view. mRNA (coral), 16S rRNA (gray) and ribosomal proteins (light blue or coloured) are in ribbon representation. The positions of mRNA nucleotides that crosslink to ribosomal proteins or eIF3 are shown as coloured spheres. colours of nucleotide positions in mRNA correspond to colours of crosslinked proteins. Light blue spheres represent nucleotides in 18S rRNA that are protected or cleaved in eIF3/40S subunit complexes.
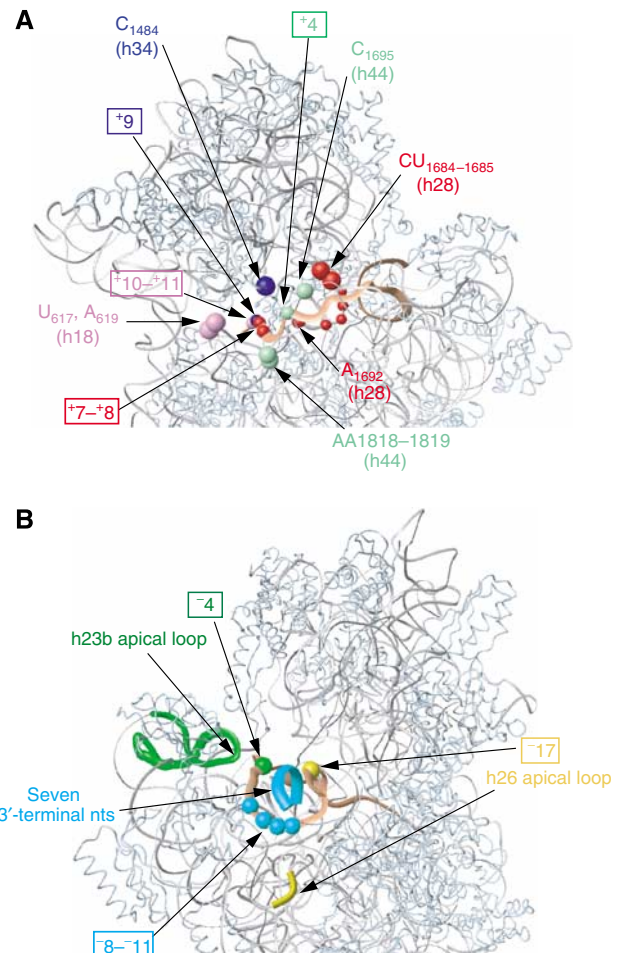

Figure 6 Nucleotides in 18S rRNA crosslinked to different positions of mRNA in 48S/80S initiation complexes mapped onto the crystal structure of the mRNA/*T. thermophilus* 30S subunit complex (Yusupova *et al*, 2006; PDB code 2HGR): (**A**) intersubunit side view and (**B**) solvent side view. mRNA (coral), 16S rRNA (gray) and ribosomal proteins (light blue) are in ribbon representation. The positions of mRNA nucleotides that crosslink to 18S rRNA are shown as coloured spheres. Crosslinked nucleotides and regions in 18S rRNA are shown as coloured spheres or segments, respectively. colours of nucleotide positions in mRNA correspond to colours of crosslinked nucleotides/segments in 18S rRNA.

h34 in the *T. thermophilus* ribosome (Yusupova *et al*, 2001) and was directly analogous to UV crosslinking of positions $^{+}11/^{+}12$ to h18 (G_{530}, A_{532}) and of positions $^{+}8/^{+}9$ to h34 (A_{1196}) in the *Escherichia coli* ribosome (Dontsova *et al*, 1992; Sergiev *et al*, 1997). This consonance suggests that mRNA nucleotides at positions $^{+}8$–$^{+}11$ are located very similarly with respect to the elements of h18 and h34 in prokaryotic ribosomes and in eukaryotic initiation complexes.

In eukaryotic initiation complexes, mRNA positions $^{+}7/^{+}8$, and particularly $^{+}7$, also crosslinked efficiently to an extensive region of h28 (nts 1684–1690 and nt 1692) with

the maximum at $CU_{1684-1685}$. However, in prokaryotes, position $^{+}7$ is close only to the equivalent of nt 1689 in the *T. thermophilus* ribosome (Yusupova *et al*, 2001) and consistently, crosslinked to the equivalent of nt 1691 in the *E. coli* ribosome (Dontsova *et al*, 1992), whereas 16S rRNA nucleotides equivalent to $CU_{1684-1685}$ of 18S rRNA and mRNA position $^{+}7$ are too far apart to be crosslinked efficiently (Yusupova *et al*, 2001). Interestingly, G_{926} of 16S rRNA (the equivalent of G_{1203}, located on the upper strand of h28 opposite $CU_{1684-1685}$; Figure 3A) is positioned to interact with the phosphate of the $^{+}1$ nt of the P-site codon in the *T. thermophilus* ribosome (Yusupova *et al*, 2001). It has therefore been suggested that interaction with G_{926} of the 3′-tail of 16S rRNA, which results in mRNA mimicry (Carter *et al*, 2000), might be important for induction of the active conformation of the 30S subunit's P-site responsible for mRNA-independent recruitment of initiator tRNA (Yusupova

et al, 2001). The observed crosslinking of mRNA positions $^+7/^+8$ to $CU_{1684-1685}$ in eukaryotic initiation complexes suggests that G_{1203} would be too distant to interact with the $^+1$ nt of the P-site codon. Importantly, crosslinking between positions $^+7-^+8$ and h28 was no longer observed in eukaryotic 80S complexes that had undergone 2–3 elongation events (Pisarev *et al*, in preparation), which indicates that in elongation complexes, G_{1203} might be able to interact with the $^+1$ nt of the P-site codon. In fact, crosslinking of the $^+1$ nt to the equivalent of rabbit G_{1203} was observed in phased human 80S ribosomal complexes (Demeshkina *et al*, 2000, 2003). The possibility that ribosomal contacts of the mRNA P-site codon differ between initiation and elongation complexes might reflect the specific needs of the eukaryotic initiation codon selection mechanism. Crystallographic studies suggest that the absence of E-site tRNA induces changes in the 30S subunit that include increased conformational flexibility of h28 (Jenner *et al*, 2005). The lack of E-site tRNA in 48S/80S initiation complexes characterized here might thus account for the observed difference. However, although the presence/absence of E-site tRNA seems to be a likely explanation, it cannot be ruled out that the presence of eIFs in 48S initiation complexes might also influence the conformation of 40S subunits, changing the position of h28 compared to its position in elongating ribosomes, and that such a change could even be preserved in 80S initiation complexes. Thus, it has recently been reported that binding of eIF1 and eIF1A to yeast 40S subunits induces opening of the entry channel 'latch' formed between h18 in the body and h34 and rpS3 in the neck, and establishment of a new connection between the head and the body likely mediated by h16 and rpS3 that also results in a slightly different conformation of the beak (Passmore *et al*, 2007).

The previously reported crosslinking of mRNA at position $^+4$ in the A site codon to C_{1696} and $AA_{1818-1819}$ in h44 of 18S rRNA (Demeshkina *et al*, 2000; Graifer *et al*, 2004; Pisarev *et al*, 2006) is also consistent with the proximity of this mRNA position to the equivalent region of 16S rRNA in *T. thermophilus* ribosomes (Yusupova *et al*, 2001) and with UV crosslinking of position $^+4$ to the equivalent of C_{1698} in *E. coli* ribosomes (Rinke-Appel *et al*, 1993). We have suggested that interaction of the $^+4$ nucleotide with $AA_{1818-1819}$ likely accounts for the $^+4$ nucleotide context rule (Pisarev *et al*, 2006). Although S12p lies directly under the $^+5/^+6$ positions of mRNA (Yusupova *et al*, 2001) and its eukaryotic homologue rpS23 has a similar location (Spahn *et al*, 2001a), and although mutations in both S12p and rpS23 affect translational fidelity (Alksne *et al*, 1993; Anthony and Liebman, 1995; Synetos *et al*, 1996), neither protein crosslinks to mRNA at this position. However, in contrast to prokaryotic ribosomal complexes, in 48S/80S initiation complexes, mRNA at positions $^+4/^+5$ crosslinked efficiently to rpS15, a homologue of S19p (this study; Pisarev *et al*, 2006). S19p is located in the head of the 30S subunit with its C-terminal tail pointing towards the interface side but not reaching the A-site codon (Wimberly *et al*, 2000). The fact that analogous crosslinking of positions $^+4-^+6$ to rpS15 was also observed in 80S complexes phased by cognate P-site tRNA (Graifer *et al*, 2004; Bulygin *et al*, 2005) suggests that crosslinking of rpS15 in initiation complexes might not be the result solely of initiation-specific conformational changes in 40S subunits (Passmore *et al*, 2007), but is likely due to N- or C-terminal

extensions in rpS15 relative to S19p, whose functional significance is presently unknown.

Taken together, our crosslinking results indicate that the overall ribosomal position of the mRNA downstream of the P-site codon in eukaryotic 48S/80S initiation complexes is similar to that of mRNA in prokaryotic 70S ribosomes. Differences include the close proximity of mRNA positions $^+7/^+8$ to the central portion of the lower strand of h28 and of positions $^+4/^+5$ to rpS15.

Ribosomal position and contacts of mRNA upstream of the P-site

The position of mRNA in eukaryotic initiation complexes upstream of the P-site is particularly interesting because eukaryotes lack the SD interaction. In eukaryotic 48S/80S initiation complexes, mRNA positions $^-3/^-4$ and $^-6/^-7$ crosslinked efficiently to rpS5 (the homologue of S7p) and rpS14 (the homologue of S11p), respectively, and position $^-4$ also crosslinked to the apex of h23b (equivalent to the 690 loop of 16S rRNA). These results are consistent with the proximity of this region of mRNA to S7p, S11p and the 690 loop of h23 in *T. thermophilus* ribosomal complexes (Yusupova *et al*, 2001) and with crosslinking of positions $^-2/^-3$ to the equivalent of rabbit G_{957} in the apex loop of H23b in phased human 80S ribosomal complexes (Demeshkina *et al*, 2000, 2003). Some of the other mRNA interactions on the E-site side of the 40S subunit are also comparable to interactions in prokaryotes. Thus, $^-8-^-11$ mRNA residues crosslinked to the 3′-terminal nts 1857–1863 of 18S rRNA, indicating that they occupy a position in eukaryotic initiation complexes analogous to the mRNA and rRNA elements of the SD duplex in prokaryotic initiation complexes despite the lack of base-pairing potential (Yusupova *et al*, 2001).

However, other upstream interactions are unique to eukaryotes. Thus, in 48S initiation complexes, mRNA position $^-3$ also specifically interacts with eIF2α (Pisarev *et al*, 2006), suggesting that in contrast to prokaryotic initiation complexes, the E-site in eukaryotic 48S complexes is partially occupied by an initiation factor, eIF2. This interaction is important for 48S complex formation in the presence of eIF1, and accounts for the $^-3$ nucleotide context rule (Pisarev *et al*, 2006). Positions $^-6$ and $^-7/^-10$ also efficiently crosslinked to eukaryote-specific rpS28 and rpS26, respectively. Crosslinking of S26 to positions $^-4-^-9$ was previously observed in phased human 80S ribosomal complexes with RNAs containing mid-range nucleotide derivatives (Graifer *et al*, 2004). The identification of rpS26 and rpS28 in contact with mRNA in the immediate vicinity of rpS14 is consistent with observations from cryo-EM analysis of yeast 40S subunits that additional protein density at the top of the platform surrounds rpS14, leading to a stronger contact of the platform with rpS5 in the head of the 40S subunit, which constitutes part of the mRNA exit channel (Spahn *et al*, 2001a).

Moreover, UV crosslinking revealed specific interactions between mRNA and two subunits of eIF3 in 48S complexes: the most intense crosslinking occurred between eIF3a and mRNA position $^-14$, whereas eIF3d crosslinked to positions $^-8-^-17$ with similar medium intensities. These data are consistent with previous reports that eIF3 can be crosslinked to β-globin mRNA in 48S complexes, that its 3d subunit is close to 18S rRNA and that binding of eIF3 to the 40S subunit

can be stabilized by mRNA (Nygård and Westermann, 1982; Westermann and Nygård, 1984; Unbehaun *et al*, 2004; Kolupaeva *et al*, 2005). They also suggest that eIF3d contributes to formation of the mRNA-binding channel on the 40S subunit itself (as positions $^{-}8$–$^{-}10$ crosslink simultaneously to eIF3d and rps), and that eIF3a likely forms a direct extension of it, which together might contribute to the processivity of scanning and stabilize 48S complexes after hydrolysis of eIF2-bound GTP but prior to subunit joining (Unbehaun *et al*, 2004). Interaction between mRNA and eIF3 in 48S complexes most likely also accounts for observations that whereas eukaryotic 80S initiation complexes protect $\sim$30 nt flanking the initiation codon from RNAse cleavage, 48S complexes protect an additional 10–18 upstream nucleotides (e.g. Kozak, 1977; Lazarowitz and Robertson, 1977). The suggested eIF3/mRNA interaction upstream of the E-site is in good agreement with models derived from cryo-EM reconstructions that located the five-lobed eIF3 on the solvent side of the 40S subunit, with its left arm pointing towards the E-site (Siridechadilok *et al*, 2005). Our crosslinking data therefore suggest that eIF3d and eIF3a likely contribute to formation of the left arm of eIF3. The specificity of eIF3/mRNA crosslinking is also consistent with the finding that the N-terminal domain of eIF3a interacts with RPS0, placing it in the vicinity of the mRNA exit channel on the solvent side of the 40S subunit (Valásek *et al*, 2003), and with the crosslinking reported here of mRNA position $^{-}17$ to U_{1107} in the eukaryote-specific expansion segment ES7 of h26 on the back of the platform (Spahn *et al*, 2001a).

Enzymatic footprinting and hydroxyl radical cleavage experiments indicate that eIF3 protects G_{537} and C_{539} in h16 from RNase T1 and RNase V1 digestion, respectively, and that it also induces cleavage by hydroxyl radicals at $GC_{537-538}$. Although hydroxyl radical cleavage indicates that eIF3 is indeed located in the vicinity of h16, it is not possible to conclude unambiguously whether protection from RNase cleavage is caused by direct contact of eIF3 with h16 or if it results from conformational changes in the 40S subunit caused by eIF3 binding. Moreover, whereas the eIF3/40S model derived from cryo-EM reconstructions does not suggest that eIF3 interacts with the shoulder (Siridechadilok *et al*, 2005), according to another report, the C-terminal domain of yeast eIF3a (TIF32) can specifically bind to a fragment of 18S rRNA encompassing h16–h18 (Valásek *et al*, 2003). In contrast to bacterial 30S subunits, in which h16 is folded towards h18, h16 in eukaryotic 40S subunits is rotated towards the back of the 40S subunit and points into the solvent (Spahn *et al*, 2001a, b; Passmore *et al*, 2007). Binding of eIF1/eIF1A, the HCV IRES and the CrPV IRES to the 40S subunit all result in opening of the entry 'latch' between h18 in the body and h34/rpS5 in the neck and concomitant establishment of a new connection between h16 and rpS3, which suggests that these ribosomal conformational changes constitute general changes that occur during initiation (Spahn *et al*, 2001b, 2004; Passmore *et al*, 2007). It is therefore likely that binding of eIF3 to 40S subunits could also result in similar changes, which might account for protection of h16 from RNase digestion.

Taken together, our crosslinking results indicate that the overall ribosomal position of mRNA upstream of the P-site codon in eukaryotic 48S/80S initiation complexes is similar to that of mRNA in prokaryotic 70S ribosomes. Differences in

mRNA contacts include interactions of eukaryotic mRNA with eIF2 in the E-site, with eukaryote-specific rpS26 and rpS28 on the platform and with eIF3 on the back of the platform. The interaction of mRNA at position $^{-}3$ with eIF2α is essential for correct initiation codon selection (Pisarev *et al*, 2006). Although it is very likely that other eukaryote-specific contacts of mRNA with 40S subunit and eIF3 that we detected in 48S complexes are employed to accommodate the eukaryote-specific initiation stages of ribosomal attachment to and scanning on mRNA, we cannot exclude that the contacts between mRNA and initiation complex constituents during attachment and scanning might differ slightly from those in the assembled 48S complexes that are reported here. We did not detect any crosslinking of mRNA with eIFs 4A/4B/4F. Although it is possible that these factors had dissociated from initiation complexes during sucrose density gradient purification, it cannot be strictly excluded that they instead interact with mRNA regions outside those investigated here or that their interactions with mRNA differ during initial attachment of 43S complexes, scanning and formation of 48S complexes.

Materials and methods

UV crosslinking experiments

48S/80S initiation complexes were assembled and purified by sucrose density gradient centrifugation essentially as described (Pisarev *et al*, 2006). Thus, to form 48S complexes, 100 ng of ^{32}P-labelled 4-thioU-containing mRNAs were incubated with 8 pmol 40S subunits, 10 pmol Met-tRNA$_i^{Met}$, 5 μg eIF2, 15 μg eIF3, 2.5 μg eIF4A, 0.5 μg eIF4B, 2.5 μg eIF4F, 0.2 μg eIF1A, 0.2 μg eIF1 in 100 μl buffer A (20 mM Tris pH 7.5, 100 mM KAc, 2 mM DTT, 2.5 mM MgAc$_2$, 0.25 mM spermidine) supplemented with 1 mM ATP and 0.4 mM GTP for 10 min at 37°C. To obtain 80S initiation complexes, 48S complexes were further incubated with 10 pmol 60S subunits, 5 μg eIF5 and 5 μg eIF5B for 10 min at 37°C. Assembled ribosomal complexes were purified by centrifugation through 10–30% sucrose density gradients prepared in buffer A in a Beckman SW55 rotor at 53 000 r.p.m. for 75 min. The presence of [^{32}P]mRNA in gradient fractions was monitored by Cherenkov counting. Equal amounts of counts ($\sim$200 000 c.p.m.) of peak fractions were irradiated at 360 nm for 30 min on ice using a UV-Stratalinker (Stratagene). After UV irradiation, 48S complexes were subjected to a second round of sucrose density gradient centrifugation.

To analyse crosslinked proteins by one-dimensional electrophoresis, crosslinked ribosomal fractions were treated with RNase A and subjected to electrophoresis in NuPAGE 4–12% Bis-Tris-Gel (Invitrogen) followed by autoradiography. UV crosslinked rps were further identified by acidic-SDS 2D gel electrophoresis exactly as described (Madjar *et al*, 1979; Pisarev *et al*, 2006). The identity of rps was confirmed by LC-nanospray tandem mass spectrometry of peptides derived by in-gel tryptic digestion at an in-house facility.

Identification of crosslinked nucleotides in 18S rRNA was done exactly as described (Pisarev *et al*, 2006). Regions of 18S rRNA crosslinked to ^{32}P-labelled mRNA were first identified by RNase H digestion of 18S rRNA hybridized with a panel of $\sim$20-mer DNA oligonucleotides complementary to different regions of 18S rRNA using a previously described strategy (Dontsova *et al*, 1992). 18S rRNA fragments were separated by electrophoresis in 12% denaturing gel. Crosslinked fragments were attributed to corresponding regions of 18S rRNA taking into account the reduced mobility of crosslinked rRNA fragments due to the covalently bound mRNA. Precise identification of crosslinked nucleotides in 18S rRNA was done by primer extension inhibition using AMV RT and primers chosen on the basis of RNase H digestion.

Chemical and enzymatic footprinting analysis of eIF3/40S subunit complexes

Binary eIF3/40S complexes were assembled by incubating 30 pmol 40S subunits, 50 pmol eIF3, 3 μg poly(U) RNA in 100 μl buffer A for 10 min at 37°C (Kolupaeva *et al*, 2005), purified by sucrose density

gradient centrifugation and then either enzymatically digested by incubation with RNase V1 (final concentration 0.9 U/ml) for 15 min at 37°C or with RNase T1 (final concentration 0.5 U/ml) for 11 min at 37°C or modified by incubation with CMCT. Cleavage/modification sites in 18S rRNA were identified by primer extension using AMV-RT.

Directed hydroxyl radical cleavage of 18S rRNA in [Fe(II)–BABE]–eIF3/40S subunit complexes

eIF3 was derivatized with Fe(II)–BABE as described (Culver and Noller, 2000; Lomakin *et al*, 2003) by incubating 300 pmol eIF3 with 1 mM Fe(II)–BABE in buffer B (80 mM HEPES pH 7.5, 100 mM KCl, 5% glycerol, 2.5 mM MgCl$_2$) for 20 min at 37°C. Fe(II)–BABE-derivatized eIF3 was separated from unincorporated Fe(II)–BABE on YM-30 microcons.

Binary [Fe(II)–BABE]–eIF3/40S subunit complexes were assembled by incubating 40 pmol 40S subunits and 50 pmol Fe(II)–BABE-derivatized eIF3 with 5 μg poly(U) RNA for 10 min at 37°C in 200 μl in buffer B. Complexes were isolated by centrifugation in a Beckman SW55 rotor for 2 h at 4°C and 42 000 r.p.m. in 10–30% linear sucrose density gradients in buffer B adjusted to 4 mM MgCl$_2$.

Gradient fractions that contained 40S subunits were analysed for the presence of eIF3 by SDS–PAGE and Coomassie staining (Kolupaeva *et al*, 2005) and used for directed hydroxyl radical probing. To generate hydroxyl radicals, the reaction mixture was supplemented with 0.025% H$_2$O$_2$ and 5 mM ascorbic acid and incubated on ice for 10 min. Reactions were quenched by addition of 10 mM thiourea. 18S rRNA was analysed by primer extension.

Construction of plasmids and methods for purification of translation components are described in Supplementary data.

References

Alksne LE, Anthony RA, Liebman SW, Warner JR (1993) An accuracy center in the ribosome conserved over 2 billion years. *Proc Natl Acad Sci USA* **90:** 9538–9541

Anthony RA, Liebman SW (1995) Alterations in ribosomal protein RPS28 can diversely affect translational accuracy in *Saccharomyces cerevisiae. Genetics* **140:** 1247–1258

Bulygin K, Chavatte L, Frolova L, Karpova G, Favre A (2005) The first position of a codon placed in the A site of the human 80S ribosome contacts nucleotide C1696 of the 18S rRNA as well as proteins S2, S3, S3a, S30, and S15. *Biochemistry* **44:** 2153–2162

Carter AP, Clemons WM, Brodersen DE, Morgan-Warren RJ, Wimberly BT, Ramakrishnan V (2000) Functional insights from the structure of the 30S ribosomal subunit and its interactions with antibiotics. *Nature* **407:** 340–348

Clemons Jr WM, May JL, Wimberly BT, McCutcheon JP, Capel MS, Ramakrishnan V (1999) Structure of a bacterial 30S ribosomal subunit at 5.5 Å resolution. *Nature* **400:** 833–840

Culver GM, Noller HF (2000) Directed hydroxyl radical probing of RNA from iron(II) tethered to proteins in ribonucleoprotein complexes. *Methods Enzymol* **318:** 461–475

Demeshkina N, Laletina E, Meschaninova M, Ven'yaminova A, Graifer D, Karpova G (2003) Positioning of mRNA codons with respect to 18S rRNA at the P and E sites of human ribosome. *Biochim Biophys Acta* **1627:** 39–46

Demeshkina N, Repkova M, Ven'yaminova A, Graifer D, Karpova G (2000) Nucleotides of 18S rRNA surrounding mRNA codons at the human ribosomal A, P, and E sites: a crosslinking study with mRNA analogs carrying an aryl azide group at either the uracil or the guanine residue. *RNA* **6:** 1727–1736

Dontsova O, Dokudovskaya S, Kopylov A, Bogdanov A, Rinke-Appel J, Jünke N, Brimacombe R (1992) Three widely separated positions in the 16S RNA lie in or close to the ribosomal decoding region; a site-directed cross-linking study with mRNA analogues. *EMBO J* **11:** 3105–3116

Favre A, Saintomé C, Fourrey JL, Clivio P, Laugâa P (1998) Thionucleobases as intrinsic photoaffinity probes of nucleic acid structure and nucleic acid–protein interactions. *J Photochem Photobiol B* **42:** 109–124

Frank J, Zhu J, Penczek P, Li Y, Srivastava S, Verschoor A, Radermacher M, Grassucci R, Lata RK, Agrawal RK (1995) A model of protein synthesis based on cryo-electron microscopy of the *E. coli* ribosome. *Nature* **376:** 441–444

Gabashvili IS, Agrawal RK, Grassucci R, Frank J (1999) Structure and structural variations of the *Escherichia coli* 30S ribosomal subunit as revealed by three-dimensional cryo electron microscopy. *J Mol Biol* **286:** 1285–1291

Graifer D, Molotkov M, Styazhkina V, Demeshkina N, Bulygin K, Eremina A, Ivanov A, Laletina E, Ven'yaminova A, Karpova G (2004) Variable and conserved elements of human ribosomes surrounding the mRNA at the decoding and upstream sites. *Nucleic Acids Res* **32:** 3282–3289

Jenner L, Rees B, Yusupov M, Yusupova G (2007) Messenger RNA conformations in the ribosomal E site revealed by X-ray crystallography. *EMBO Rep* **8:** 846–850

Jenner L, Romby P, Rees B, Schulze-Briese C, Springer M, Ehresmann C, Ehresmann B, Moras D, Yusupova G, Yusupov M (2005) Translational operator of mRNA on the ribosome: how repressor proteins exclude ribosome binding. *Science* **308:** 120–123

Kolupaeva VG, Unbehaun A, Lomakin IB, Hellen CU, Pestova TV (2005) Binding of eukaryotic initiation factor 3 to ribosomal 40S subunits and its role in ribosomal dissociation and anti-association. *RNA* **11:** 470–486

Korostelev A, Trakhanov S, Asahara H, Laurberg M, Lancaster L, Noller HF (2007) Interactions and dynamics of the Shine Dalgarno helix in the 70S ribosome. *Proc Natl Acad Sci USA* **104:** 16840–16843

Kozak M (1977) Nucleotide sequences of 5'-terminal ribosome-protected initiation regions from two reovirus messages. *Nature* **269:** 391–394

Kozak M (1991) Structural features in eukaryotic mRNAs that modulate the initiation of translation. *J Biol Chem* **266:** 19867–19870

Lazarowitz SG, Robertson HD (1977) Initiator regions from the small size class of reovirus messenger RNA protected by rabbit reticulocyte ribosomes. *J Biol Chem* **252:** 7842–7849

Lomakin IB, Kolupaeva VG, Marintchev A, Wagner G, Pestova TV (2003) Position of eukaryotic initiation factor eIF1 on the 40S ribosomal subunit determined by directed hydroxyl radical probing. *Genes Dev* **17:** 2786–2797

Lomakin IB, Shirokikh NE, Yusupov MM, Hellen CUT, Pestova TV (2006) The fidelity of translation initiation: reciprocal activities of eIF1, IF3 and YciH. *EMBO J* **25:** 196–210

Madjar JJ, Arpin M, Buisson M, Reboud JP (1979) Spot position of rat liver ribosomal proteins by four different two-dimensional electrophoreses in polyacrylamide gel. *Mol Gen Genet* **171:** 121–134

Nygård O, Westermann B (1982) Specific interaction of one subunit of eukaryotic initiation factor eIF-3 with 18S ribosomal RNA within the binary complex, eIF-3 small ribosomal subunit, as shown by cross-linking experiments. *Nucleic Acids Res* **10:** 1327–1334

Passmore LA, Schmeing TM, Maag D, Applefield DJ, Acker MG, Algire MA, Lorsch JR, Ramakrishnan V (2007) The eukaryotic translation initiation factors eIF1 and eIF1A induce an open conformation of the 40S ribosome. *Mol Cell* **26:** 41–50

Pestova TV, Kolupaeva VG (2002) The roles of individual eukaryotic translation initiation factors in ribosomal scanning and initiation codon selection. *Genes Dev* **16:** 2906–2922

Pestova TV, Lorsch JR, Hellen CUT (2007) *The Mechanism of Translation Initiation in Eukaryotes*, pp 87–128. Cold Spring Harbor, NY: Translational Control in Biology and Medicine, Cold Spring Harbor Laboratory Press

Pisarev AV, Hellen CUT, Pestova TV (2007) Recycling of eukaryotic posttermination ribosomal complexes. *Cell* **131:** 286–299

Pisarev AV, Kolupaeva VG, Pisareva VP, Merrick WC, Hellen CUT, Pestova TV (2006) Specific functional interactions of nucleotides at key −3 and +4 positions flanking the initiation codon with components of the mammalian 48S translation initiation complex. *Genes Dev* **20:** 624–636

Rinke-Appel J, Jünke N, Brimacombe R, Dukudovskaya S, Dontsova O, Bogdanov A (1993) Site-directed cross-linking of mRNA analogues to 16S ribosomal RNA; a complete scan of cross-links from all positions between ' + 1' and ' + 16' on the mRNA, downstream from the decoding site. *Nucleic Acids Res* **21:** 2853–2859

Schluenzen F, Tocilj A, Zarivach R, Harms J, Gluehmann M, Janell D, Bashan A, Bartels H, Agmon I, Franceschi F, Yonath A (2000) Structure of functionally activated small ribosomal subunit at 3.3 angstroms resolution. *Cell* **102:** 615–623

Selmer M, Dunham CM, Murphy IV FV, Weixlbaumer A, Petry S, Kelley AC, Weir JR, Ramakrishnan V (2006) Structure of the 70S ribosome complexed with mRNA and tRNA. *Science* **313:** 1935–1942

Sergiev P, Leonov A, Dokudovskaya S, Shpanchenko O, Dontsova O, Bogdanov A, Rinke-Appel J, Mueller F, Osswald M, von Knoblauch K, Brimacombe R (2001b) Correlating the X-ray structures for halo- and thermophilic ribosomal subunits with biochemical data for the *Escherichia coli* ribosome. *Cold Spring Harb Symp Quant Biol* **66:** 87–100

Sergiev PV, Dontsova OA, Bogdanov AA (2001a) Study of ribosome structure using the biochemical methods: judgment day. *Mol Biol (Mosk)* **35:** 559–583

Sergiev PV, Lavrik IN, Wlasoff VA, Dokudovskaya SS, Dontsova OA, Bogdanov AA, Brimacombe R (1997) The path of mRNA through the bacterial ribosome: a site-directed crosslinking study using new photoreactive derivatives of guanosine and uridine. *RNA* **3:** 464–475

Siridechadilok B, Fraser CS, Hall RJ, Doudna JA, Nogales E (2005) Structural roles for human translation factor eIF3 in initiation of protein synthesis. *Science* **310:** 1513–1515

Spahn CM, Beckmann R, Eswar N, Penczek PA, Sali A, Blobel G, Frank J (2001a) Structure of the 80S ribosome from *Saccharomyces cerevisiae*—tRNA-ribosome and subunit–subunit interactions. *Cell* **107:** 373–386

Spahn CM, Jan E, Mulder A, Grassucci RA, Sarnow P, Frank J (2004) Cryo-EM visualization of a viral internal ribosome entry site bound to human ribosomes: the IRES functions as an RNA-based translation factor. *Cell* **118:** 465–475

Spahn CM, Kieft JS, Grassucci RA, Penczek PA, Zhou K, Doudna JA, Frank J (2001b) Hepatitis C virus IRES RNA-induced changes in the conformation of the 40S ribosomal subunit. *Science* **291:** 1959–1962

Synetos D, Frantziou CP, Alksne LE (1996) Mutations in yeast ribosomal proteins S28 and S4 affect the accuracy of translation and alter the sensitivity of the ribosomes to paromomycin. *Biochim Biophys Acta* **1309:** 156–166

Unbehaun A, Borukhov SI, Hellen CU, Pestova TV (2004) Release of initiation factors from 48S complexes during ribosomal subunit joining and the link between establishment of codon–anticodon base-pairing and hydrolysis of eIF2-bound GTP. *Genes Dev* **18:** 3078–3093

Unbehaun A, Marintchev A, Lomakin IB, Didenko T, Wagner G, Hellen CU, Pestova TV (2007) Position of eukaryotic initiation factor eIF5B on the 80S ribosome mapped by directed hydroxyl radical probing. *EMBO J* **26:** 3109–3123

Valásek L, Mathew AA, Shin BS, Nielsen KH, Szamecz B, Hinnebusch AG (2003) The yeast eIF3 subunits TIF32/a, NIP1/c, and eIF5 make critical connections with the 40S ribosome *in vivo*. *Genes Dev* **17:** 786–799

Westermann P, Nygård O (1984) Cross-linking of mRNA to initiation factor eIF-3, 24 kDa cap binding protein and ribosomal proteins S1, S3/3a, S6 and S11 within the 48S pre-initiation complex. *Nucleic Acids Res* **12:** 8887–8897

Wimberly BT, Brodersen DE, Clemons Jr WM, Morgan-Warren RJ, Carter AP, Vonrhein C, Hartsch T, Ramakrishnan V (2000) Structure of the 30S ribosomal subunit. *Nature* **407:** 327–339

Yusupova G, Jenner L, Rees B, Moras D, Yusupov M (2006) Structural basis for messenger RNA movement on the ribosome. *Nature* **444:** 391–394

Yusupova GZ, Yusupov MM, Cate JH, Noller HF (2001) The path of messenger RNA through the ribosome. *Cell* **106:** 233–241